energies

MDPI

Article

The Effect of Geometry on the Yield of Fresh Water from Single Slope Solar Stills

Djamal Eddine Benhadji Serradj, Timothy Anderson * and Roy Nates

Department of Mechanical Engineering, Auckland University of Technology, Auckland 1010, New Zealand
* Correspondence: timothy.anderson@aut.ac.nz; Tel.: +64-9921-9999 (ext. 8075)

Abstract: When examining the research literature relating to single slope solar stills it is apparent that much of the work has been conducted in an ad-hoc manner. This has led to several recommendations relating to the geometry of stills having developed that do not appear to have a sufficient evidentiary basis. To address this issue, this study used computational fluid dynamics simulations to examine the natural convection in single slope solar stills with cover angles between 0° and 60° and aspect ratios ranging from 1 to 8, with the results validated experimentally. Treating cover angle and aspect ratio as independent design variables showed that there are some features of the natural convection flow that account for the variation in yields reported in the literature (transitions between uni- and multi-cellular flow). More specifically, it was shown that the geometric effects could be correlated in the form of a generalized relationship and that this was able to predict the yield from several independent solar stills reported in the literature. As such, the use of the relationship will allow single slope solar stills designers to predict their yield far more accurately than is currently possible.

Keywords: natural convection; single slope solar still; geometry; cover angle; aspect ratio

Citation: Serradj, D.E.B.; Anderson, T.; Nates, R. The Effect of Geometry on the Yield of Fresh Water from Single Slope Solar Stills. *Energies* **2022**, *15*, 7244. https://doi.org/10.3390/en15197244

Academic Editor: Gianpiero Colangelo

Received: 29 August 2022
Accepted: 27 September 2022
Published: 2 October 2022

1. Introduction

Single slope solar stills are one of the oldest, simplest, and most widely researched water desalination technologies [1,2]. Given their pervasiveness, they frequently serve as a basis for comparison with other designs, while also having been the subject of numerous investigations aimed at increasing their yield by varying their geometry, absorber, glazing and insulation materials [3–10].

However, to investigate the performance of any solar distillation system, characterizing the transport processes in them is the first step in parametrically analyzing their productivity [11]. In considering the transport mechanisms taking place in solar stills, special consideration has been earmarked to the heat and mass transfer exchange between the water basin and the glass cover, as this determines the still's yield. This is because, in passive stills, natural convection is responsible for the transport of the water evaporated in the basin to the cool inclined cover. In turn the heat transfer associated with the natural convection and the evaporation are intrinsically linked. This flows through into mass transfer by virtue of the analogy between the two mechanisms. Because of this link, an improved understanding of the natural convective heat transfer has formed the basis of many studies looking to determine or improve the yield of single slope solar stills.

One of the oldest and most widely used approaches to describe the exchange between the glass cover and water basin is a relationship developed by Dunkle [12]. This equation has been extensively used [13–26] to estimate the convective heat (and mass) transfer coefficient in single slope solar stills. However, when examining the secondary reference upon which it was developed [27], it is apparent that the relationship applies to natural convection heat transfer occurring between two parallel horizontal surfaces. In this respect it is a poor representation of the geometry seen in a typical single slope solar still, and thus limits the ability to undertake a systematic analysis of single slope solar stills.

Since Dunkle's relationship was developed, numerous researchers have noted that it provided a poor prediction of the yield from their solar stills, without necessarily engaging with the principal assumptions built into it. Rather, to overcome the shortcomings of Dunkle's relationship, numerous variations and 'corrections' have been developed over the years [28–37]. Often, these studies have used experimental testing under uncontrolled conditions (e.g., outdoor testing of a single still design), and have explored a limited set of physical design parameters.

One of the challenges that arises from these studies are the widely different, and often conflicting conclusions drawn about the optimum cover angle [31], and to a lesser extent the aspect ratio (the ratio of the basin width to the average height of the still's inclined cover). For instance, numerous researchers have suggested that the cover angle of the single slope solar still should be equal to the latitude of the case study location [33,38–42]. However, the rationale to support this assertion (the rule of thumb that a solar collector should be inclined at an angle equal to its operational latitude) appears to be unfounded, as the primary absorber surface in a solar still is the horizontal basin, not the inclined absorber of a typical solar collector. As a case in point, some of the studies recorded in [43,44] show a clear disparity between the optimum inclination angle and the latitude of the location under consideration.

Given the extensive research that has been undertaken into single slope solar stills, it is surprising that there is no clear distinction between the effect that the cover inclination angle and the aspect ratio have on a still's yield. Where an attempt has been made to consider the aspect ratio or cover angle, it is apparent that the studies tend to treat the effect of cover angle and aspect ratio as a single entity. As such, they do not show the effect of either parameter independently, despite it being known that natural convection inside enclosures is strongly linked to their shape. Consequently, the correlations currently used in analyzing solar stills are limited in their ability to predict the yield of single slope solar stills for a wide range of geometries.

The present study therefore attempts to generalize these parameters in order quantify the relationship between the natural convection, the single slope solar still aspect ratio, the cover angle, and the single slope solar stills' freshwater production. This will allow future researchers and practitioners to undertake systematic parametric design analyses, and optimization, of the productivity of single slope solar stills more accurately than is currently possible.

2. Method

In the preceding section, it was noted that heat and mass transfer are intrinsically linked, and that there exists an analogy between the two. Given this link, it is possible to use an understanding of the natural convection heat transfer to inform the mass transfer in a solar still. Hence, to develop an understanding of the natural convection heat transfer inside single slope solar stills, steady-state simulations were performed using ANSYS's commercial computational fluid dynamics (CFD) software, FLUENT 19.2. CFD has proven to be a powerful tool for obtaining reliable results when dealing with natural convection flow inside enclosures and has been extensively utilised in single slope solar still studies due to its low cost compared to performing real experiments [31,32,45–47]. Moreover, it allows testing to be undertaken over a wider range of parameters than would be feasible (and that have been reported) experimentally.

Determination of natural convection heat transfer coefficients in 3D geometries using CFD can be complex due to the difficulty of convergence and the high computational cost [48]. Therefore, most studies assume 2D planar geometries when dealing with solar still-like problems. This assumption was made in this study noting that single slope solar stills are typically quite long, relative to their breadth, and their geometry does not vary along the length of the still.

The fluid modelled in the simulation was assumed to be an incompressible ideal gas with the physical properties of humid air. It was assumed that the floor of the enclosure

was heated with a constant temperature, while the inclined wall (the still cover) was cooled at a constant temperature as shown in Figure 1. Furthermore, under ideal conditions a solar still's side walls are well insulated, hence the side walls in the simulation were assumed to be adiabatic [31,34,49,50].

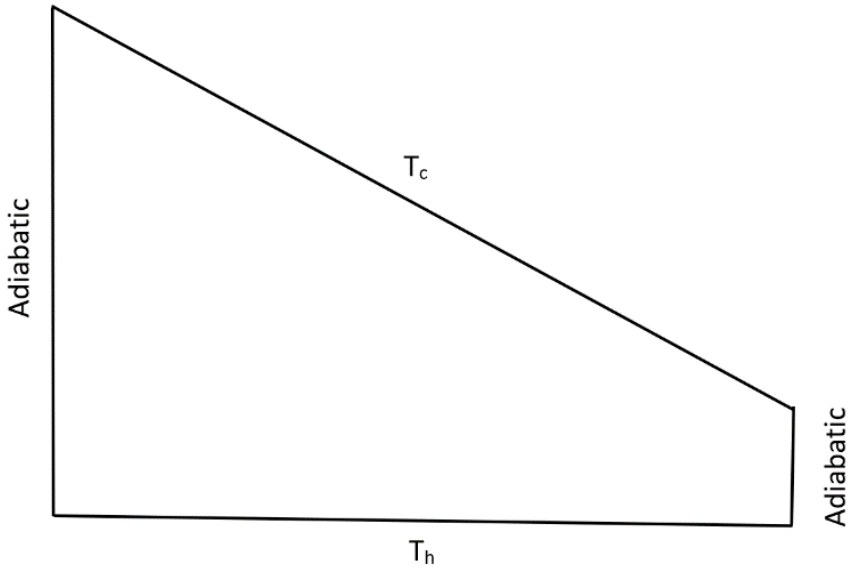

Figure 1. Boundary conditions used in this study.

Now, in a previous experimental investigation of the flow patterns inside a double slope solar still type geometry [51] it was found that the transition to turbulence occurred at approximatively Ra = 0.7×10^5. Similarly, an investigation of natural convection in a triangular enclosure (similar to a single slope solar still geometry) using flow visualization found that the flow was turbulent at Ra = 4.7×10^8 [52]. Hence, this study considered the flow to be turbulent since the range of Rayleigh numbers was between 3.37×10^6 and 3.03×10^9. As research has shown that the Realisable k-ε model exhibits excellent performance when dealing with natural convection in enclosures [48,53], it was used to resolve the turbulence field in this study. In addition, the discretized form of the continuity equations, were resolved using a coupled algorithm to handle the pressure–velocity coupling. The convection–diffusion terms were solved using a second order upwind approach, and, since the temperature changes in the working fluid were small, the Boussinesq approximation was applied in the treatment of the buoyancy. In solving these equations, a solution was assumed to have been reached when the residuals of the equations were lower than 10^{-5}.

In exploring the effect of geometry on the heat transfer, simulations were performed for a range of aspect ratios (B/L = 1–8) and inclination angles of the cover relative to the horizontal (θ = 0°–60°), with each parameter varied independently, as shown in Figure 2. Although it may seem infeasible to consider single slope solar stills with low cover inclination angles such as 0° < θ < 10° (due to the possibility of condensed water droplets falling back into the brackish water basin) some studies have considered solar stills with external condensers and lower angles, down to an inclination angle of 0° [54], and so these conditions were included in this work too.

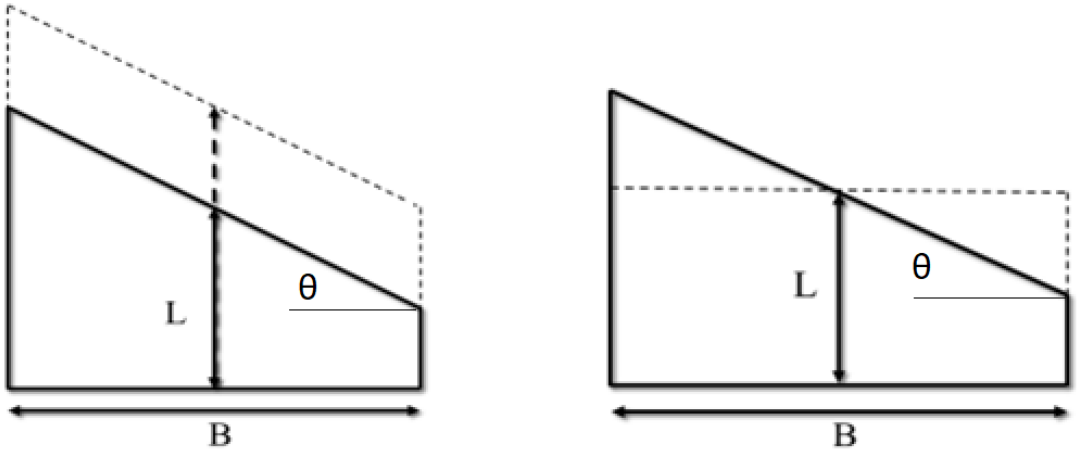

Figure 2. Single slope solar still geometry variation.

Given the spatial discretization used in CFD, it was crucial to perform a mesh sensitivity, and mesh independence, analysis to minimize the simulation time without decreasing the accuracy of the results. The grid used was structured with primarily quadrilateral elements and a smaller number of triangular elements (because of the angle in the enclosure) as shown in Figure 3.

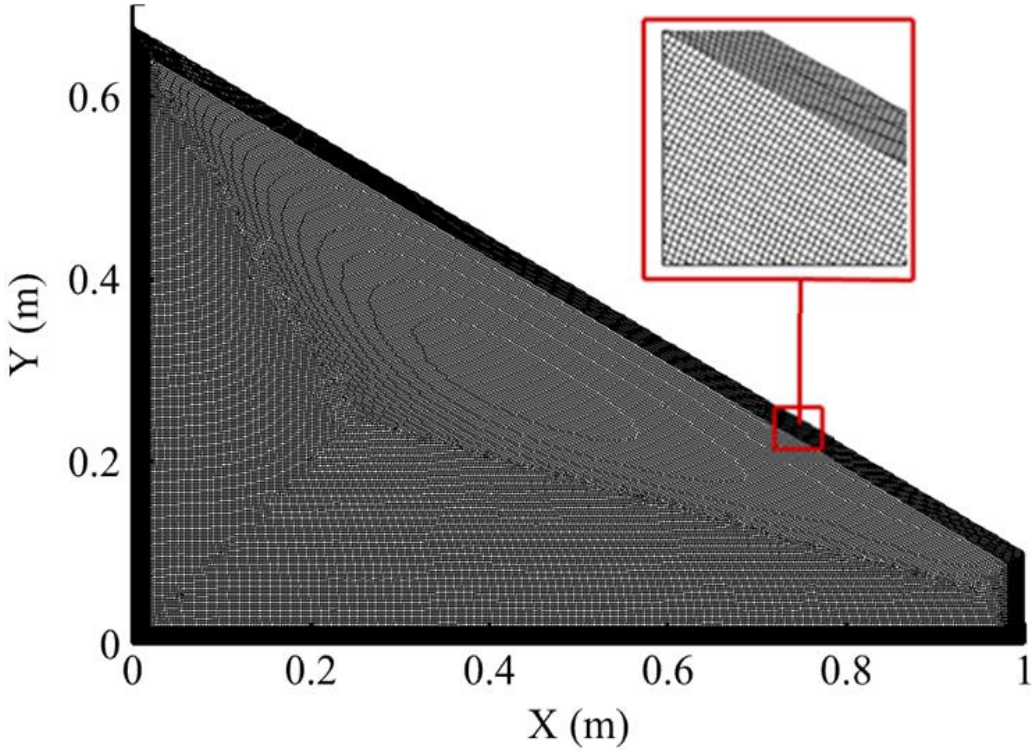

Figure 3. Computational mesh used in this study.

Twenty inflation layers were used, with a growth ratio of 1.05, to capture the boundary layer. Moreover, to ensure the correct treatment of the viscous sublayer, the distance between the wall and the first node of the grid was varied until the y + value was approximatively equal to 1 [48,55].

Additionally, the convective heat transfer coefficient at the hot surface was examined for a range of mesh sizes to determine when they became independent of the element size. Since the hot surface area was kept constant, the latter coefficient depends on the total heat flux of the hot surface, and the temperature difference between the hot and cold

surface (Equation (1)). In Figure 4 it is apparent that there was no significant change to the heat transfer coefficient for elements smaller than 0.002 m, for all angles. Given this mesh independence, this configuration was used for the study.

$$h_{cv} = \frac{q_h}{T_h - T_c} \quad (1)$$

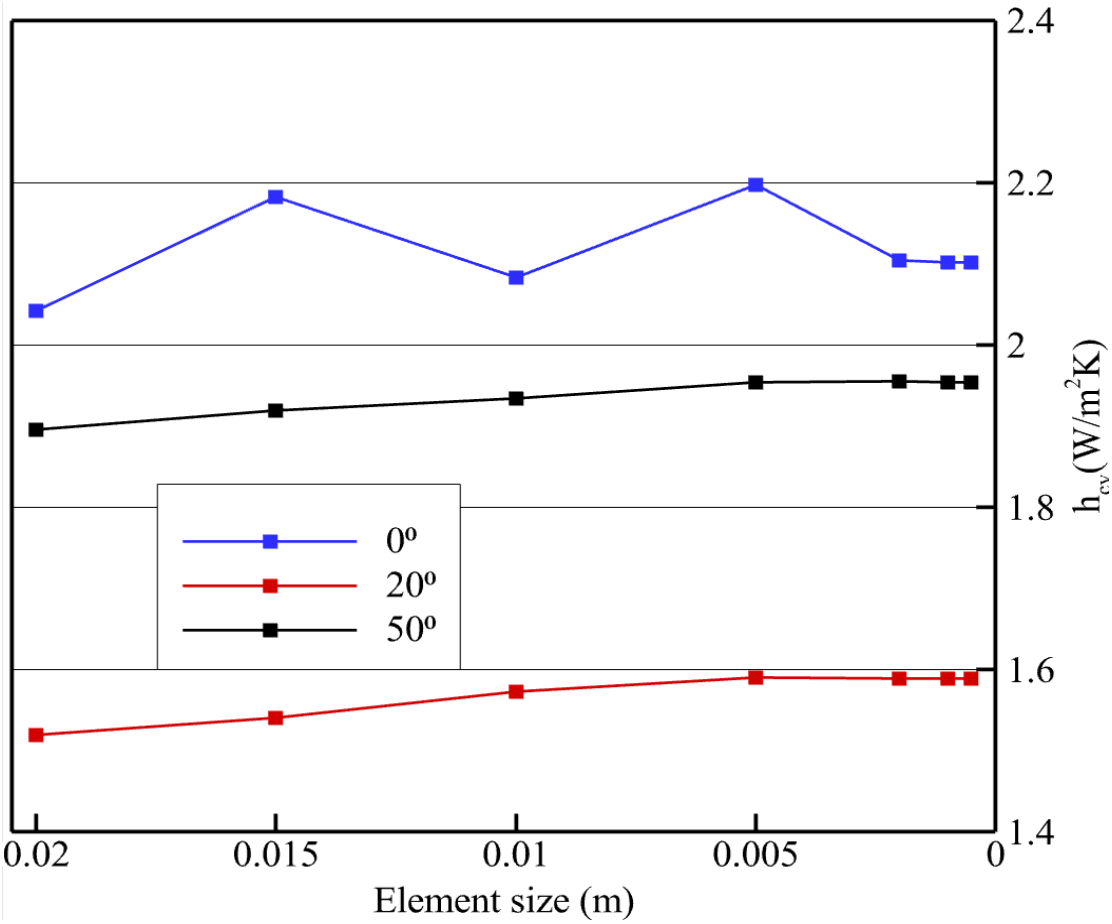

Figure 4. Variation of heat transfer coefficient with element size.

3. Validation

Before undertaking a full CFD analysis of a solar still, it was necessary to undertake a validation of the modelling methodology. To achieve this, particle image velocimetry (PIV) was used to investigate the flow inside a typical solar still geometry. Now, under typical conditions in solar stills, saturated air transports water vapor from the basin (where solar radiation is absorbed) to the cover (where the water is condensed) by natural convection. However, to ease the use of PIV in the validation experiment, silicon oil (100 cSt) was used as an analogue to this moist air in an operational still.

Despite this difference in transport media, the dimensions of the experiment and the silicone oil properties were matched such that the Rayleigh number (Equation (2)) in the experiments fell within the range of Rayleigh numbers likely to be encountered in normal single slope solar still operating conditions. To this end, an experimental single slope solar still-like geometry was fabricated with a 0.4 m × 0.4 m base (B × W), and back and front wall heights of 0.331 m and 0.1m respectively, giving a cover inclination of 30°, as shown in Figure 5.

$$Ra_s = \frac{\rho_s{}^2 g \beta_s (T_h - T_c) Cp_s L^3}{\lambda_s \mu_s} \quad (2)$$

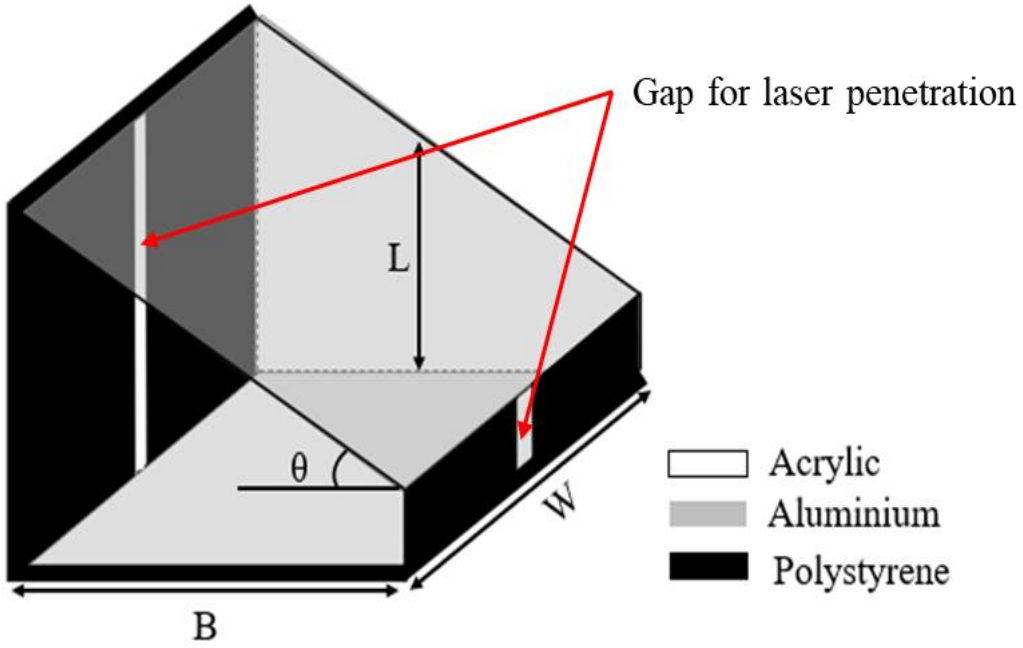

Figure 5. Schematic representation of experimental enclosure.

In fabricating the experiment, the back, front, and side walls of the still enclosure were made of transparent acrylic sheets to allow optical access. The front and back walls were insulated by a polystyrene sheet of 4 cm thickness, with a small gap was left to allow the laser sheet penetration in the cavity. However, the side walls were not insulated as optical access for the camera used in the PIV needed to be maintained. Both the cover and bottom surfaces were made from aluminum sheets of 3 mm thickness to ensure a uniform temperature distribution (and structural integrity) and were coated with black paint to avoid laser reflection.

To generate the natural convection, an adhesive aluminum foil electrical heating element (120 W) was adhered to the bottom surface of the enclosure to act as the high temperature source in the still, thus replicating the absorption of solar radiation in the basin. The heating element was connected to a Variac to control the power supplied, and thus the temperature. Again, a polystyrene sheet of 4 cm thickness was used to avoid bottom heat losses from the heating element.

To maintain a temperature difference across the still, an electric fan was used to continuously circulate ambient air over the cover and ensure a consistent temperature condition. Copper-Constantan (T-type) thermocouples were used to measure the average temperatures of both the bottom surface and the top cover, with the readings recorded using a multi-channel data logger. Sixteen thermocouples were used in the experiment; seven of them were attached to the bottom (heated) surface, seven to the cover surface, and two mounted in the ambient air.

Once the system reached steady state (typically 15 h after start-up, as shown in Figure 6) PIV measurements were undertaken. To elucidate the flow in the still, a Microvec PIV system was used to perform this study. PIV technology is a powerful tool for measuring flow velocity in cross-sectional areas, allowing the calculation of velocity fields by determining the distance travelled by illuminated particles in a time interval Δt [56]. In this work, round polyamide particles with a diameter of 50-micrometres were used to track the fluid flow inside the cavity as their low gravitational induced velocity and relaxation time made them neutrally buoyant in silicone oil.

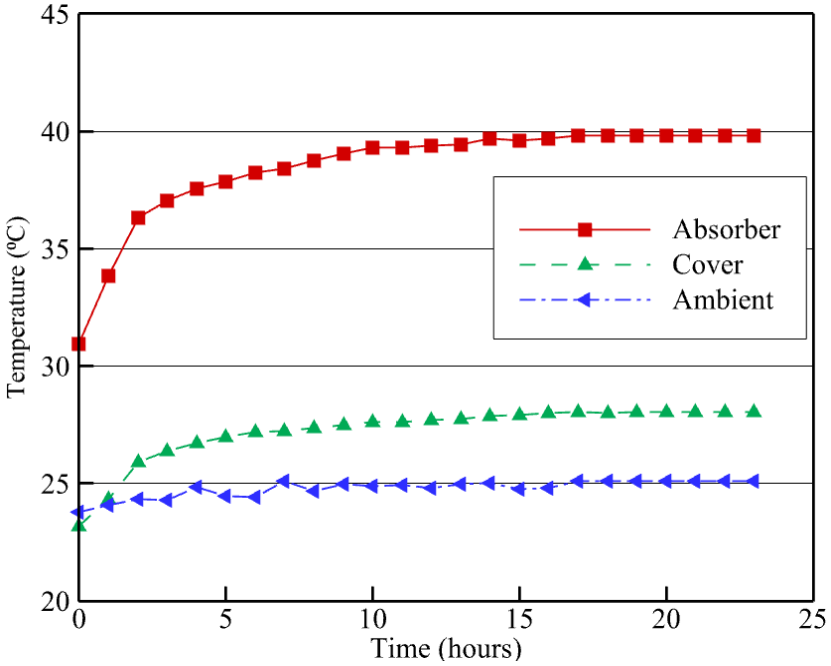

Figure 6. Experimental temperature development to steady-state.

The PIV measurement system consisted of a charge-coupled device (CCD) camera and a dual-pulse PIV laser, synchronized by using a MicroPulse725 synchronizer as shown in Figure 7. The camera recorded pairs of images (2456 × 2048 pixels) at a frame rate of 16 frames per second and a pulse delay of 40ms. To obtain a satisfactory time-averaged velocity field from the PIV 800 pairs of images were acquired at steady state conditions for analysis using the PIVLab package integrated in MATLAB (each pair of images was taken with an interval of Δt = 15 ms).

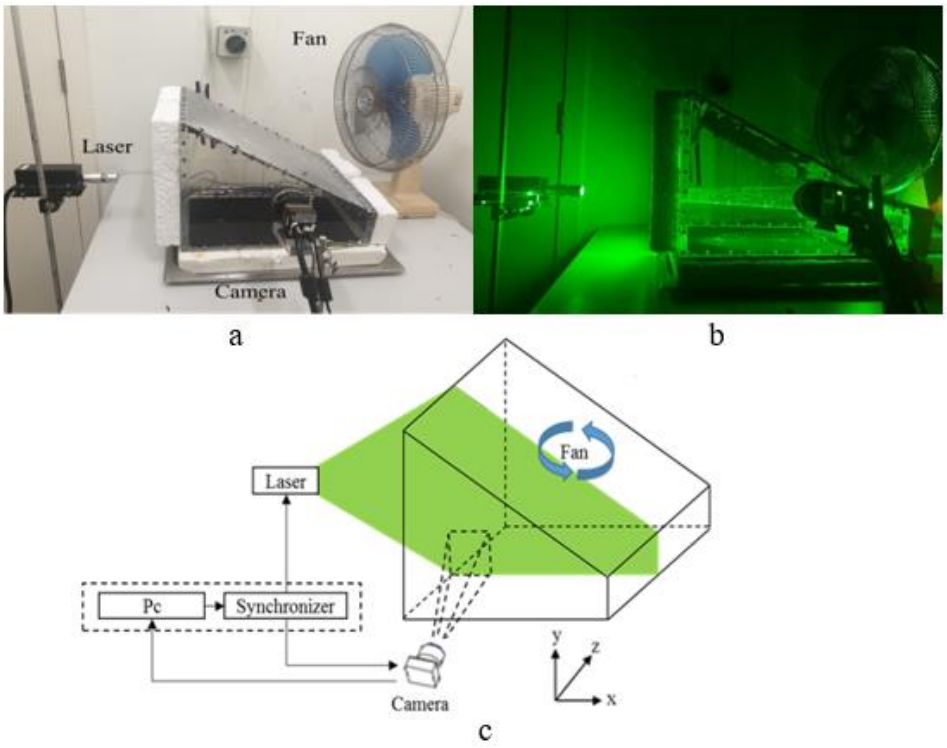

Figure 7. (**a**) Experimental set up (**b**) Laser imaging; and (**c**) Experimental schematic.

Having outlined the physical setup of the validation experiment, the experimental boundary conditions for a steady-state experimental condition were applied to a CFD simulation. The results of both the PIV experiment and the CFD simulation can be seen in Figure 8 which shows the velocity contours for both the PIV experiment and the CFD simulation at a plane 0.2 m along the still's length (i.e., in the z-direction). In both cases it is apparent (qualitatively) that there is a plume rising from the hot surface that splits the flow in the enclosure into two cells at approximately the same location.

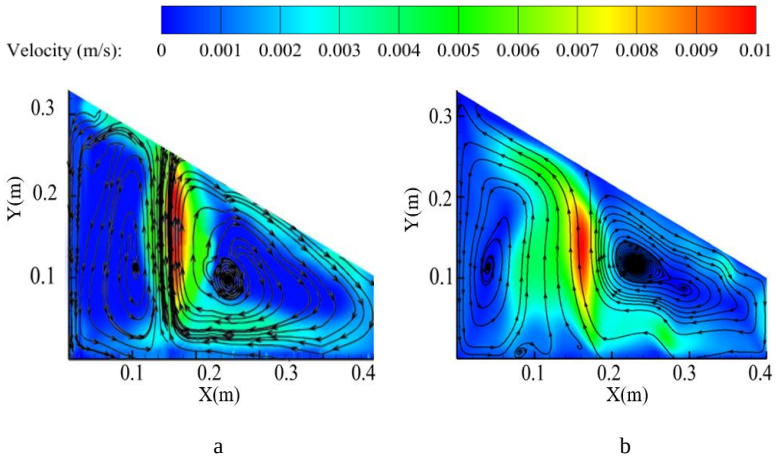

Figure 8. Cross-sectional velocity contour in the middle of the geometry (0.2 m, AR = 2.6, θ = 30°, Ra_s = 1.38 × 108), (**a**) experiment, (**b**) CFD simulation.

Examining this in more detail, a comparison of the velocity profiles across both the CFD simulation and the PIV experiment at the mid-height of the enclosure (Y = 0.16 m) was undertaken, as shown in Figure 9. Near the walls, both the simulation and measurements show that the velocity is very low compared to the velocity of the rising plume, and in general, the results from the simulations agree very well with the PIV measurements which gives confidence to the use of the CFD model. Although one may argue that the simulated plume is slightly wider than the experiment this can be attributed to the limited number of particles in the experimental study (particles at the density of the CFD mesh would impair optical access).

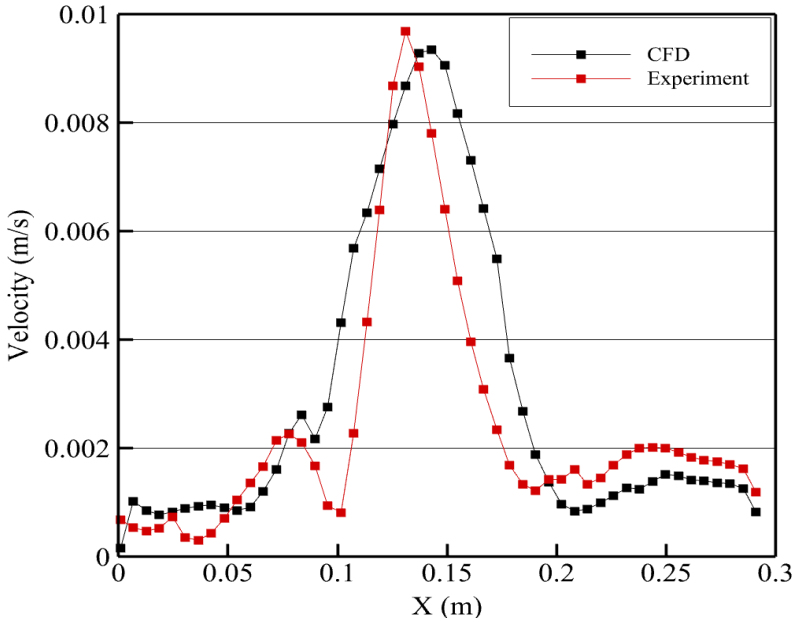

Figure 9. Velocity profile at Y = 0.16 m.

4. Results and Discussion

Having validated the use of CFD for predicting the flow in a solar still type enclosure, it was decided to examine how variations in the geometry, principally the still's aspect ratio and cover angle would change the behavior of an ideal still.

4.1. Effect of Aspect Ratio

A preliminary examination of the results found that, for a given cover angle, high heat transfer coefficients occurred at low aspect ratios, with these decrease to a minimum before again increasing, as the heat transfer mechanism moves from a conduction to convection dominated regime. This mirrors behavior often seen in double-glazing and solar water heaters. As shown in Figure 10, the local velocity at the average enclosure height varies with the aspect ratio. In particular, the velocity increases with a decrease in aspect ratio, and in turn helps explain the increased heat transfer coefficients observed at low aspect ratios.

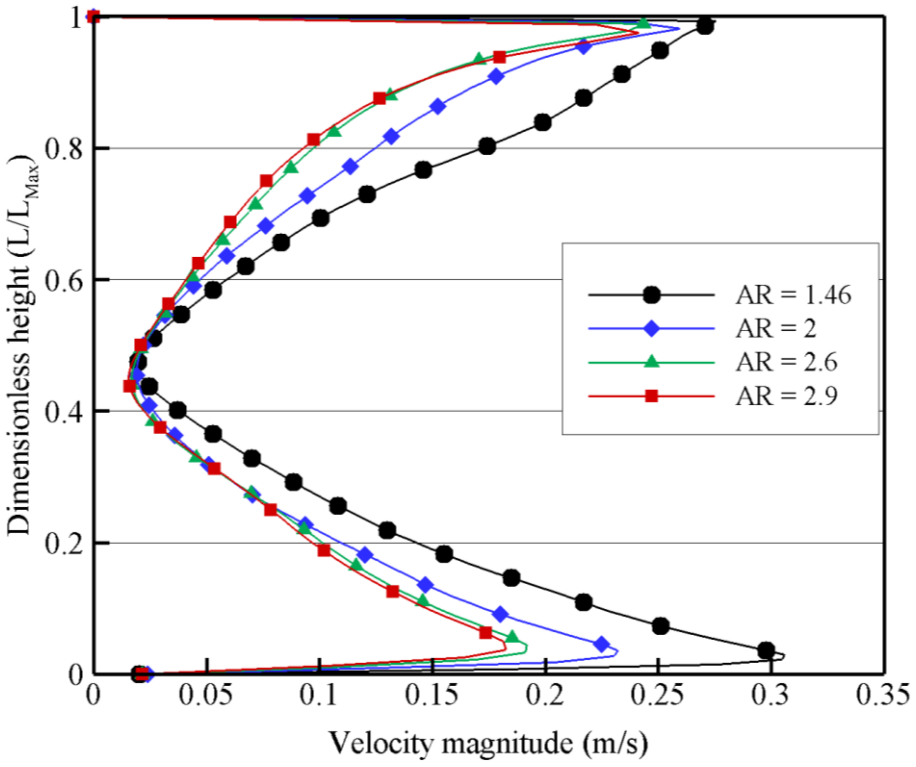

Figure 10. Local velocity at θ = 30° for different aspect ratios.

However, examining this more closely, it is worth noting that at high aspect ratios the cover surface is situated closer to the bottom surface (in a relative sense). As shown in Figure 11, this can lead to the formation of a secondary cell, with a relatively high velocity, forming near over the basin surface. This relatively high velocity flow results in an increased local heat transfer coefficient from the bottom hot surface as seen in Figure 12.

This suggests that aspect ratio plays a more important role in the natural convection transporting water from the basin to the cover in solar stills than has been recognized in the literature to date. Moreover, it shows that there are modes within the flow that may support, or inhibit, the mass transfer from the basin.

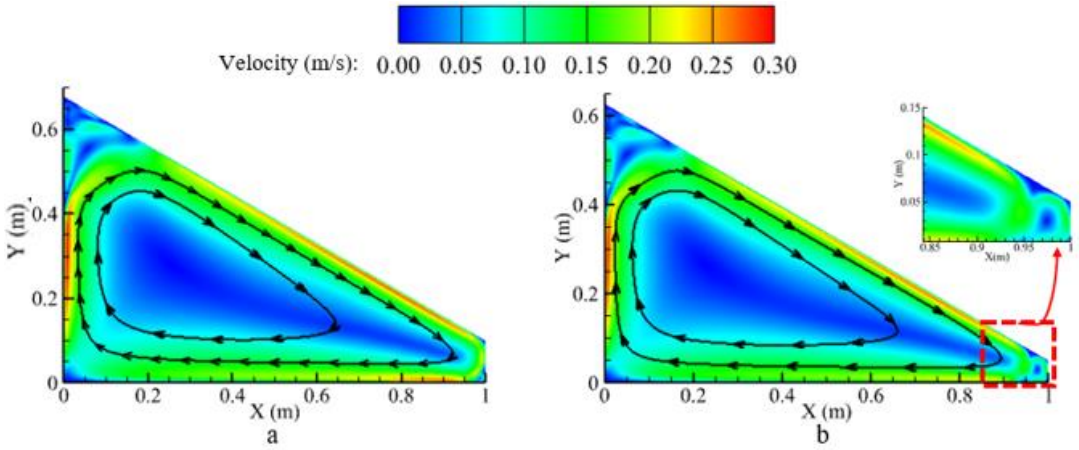

Figure 11. Streamlines at θ = 30°, (**a**) AR = 2.6, (**b**) AR = 2.9.

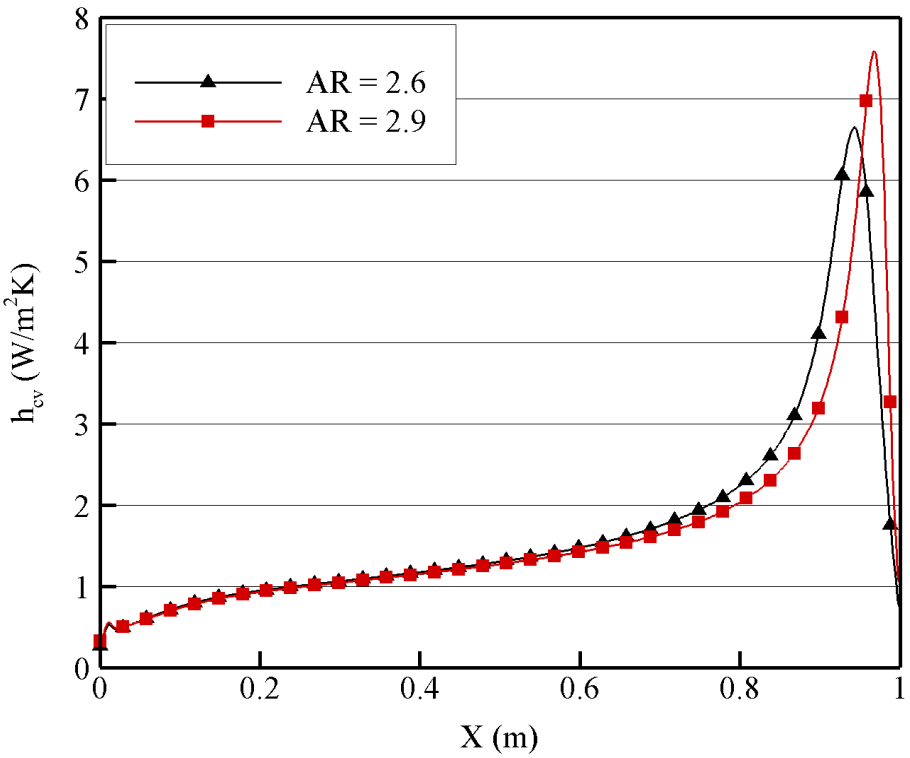

Figure 12. Convective heat transfer coefficient at θ = 30°, AR = 2.6, AR = 2.9.

4.2. Effect of Cover Angle

Having seen that aspect ratio has a role in determining the heat transfer in a single slope solar still, it is important to explore the effect that the cover angle plays on this too. Again, a preliminary examination of the results found that, for a given aspect ratio, the heat transfer coefficient from the basin typically increased with an increase in the cover angle. An exception to this is a still with a high aspect ratio (AR = 5.52), whereby the heat transfer coefficient initially decreases for a change in cover angle from 0° to 10°.

To explain the variation in the heat transfer coefficient at AR = 5.52, it is necessary to look at Figure 13 for two different angles (θ = 0°, b: θ = 10°). From this it is apparent that at lower angles (θ = 0°) there are multiple cells (Bénard cells), whereas at θ = 10° there is a single cell. The presence of multiple cells allows more heat (or water) to be carried away from the bottom surface (the basin). Further illustrating this point, Figure 14 shows the effect of the cover angle on the local heat transfer coefficient from the bottom hot surface. At a low aspect angle (θ = 10°), the heat transfer coefficient reaches a peak twice (x = 0.05 m

and x = 0.8 m) because of the formation of three cells. However, at a higher cover angle (θ = 10°) the heat transfer coefficient reaches its peak at the low wall where cold fluid begins transporting heat from the bottom wall, in a single cell pattern. Even though the peak for θ = 10° is higher than the two peaks for θ = 0°, the overall heat transfer coefficient is higher in the latter case. This is because the multi-cellular flow, is more efficient at transporting heat away from the hot basin surface.

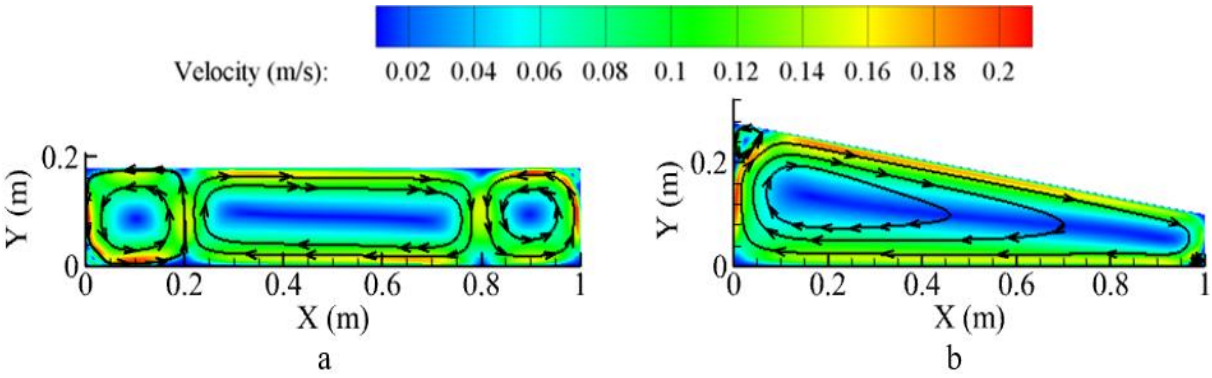

Figure 13. Velocity streamlines at AR = 5.52; (**a**) θ = 0°, (**b**) θ = 10°.

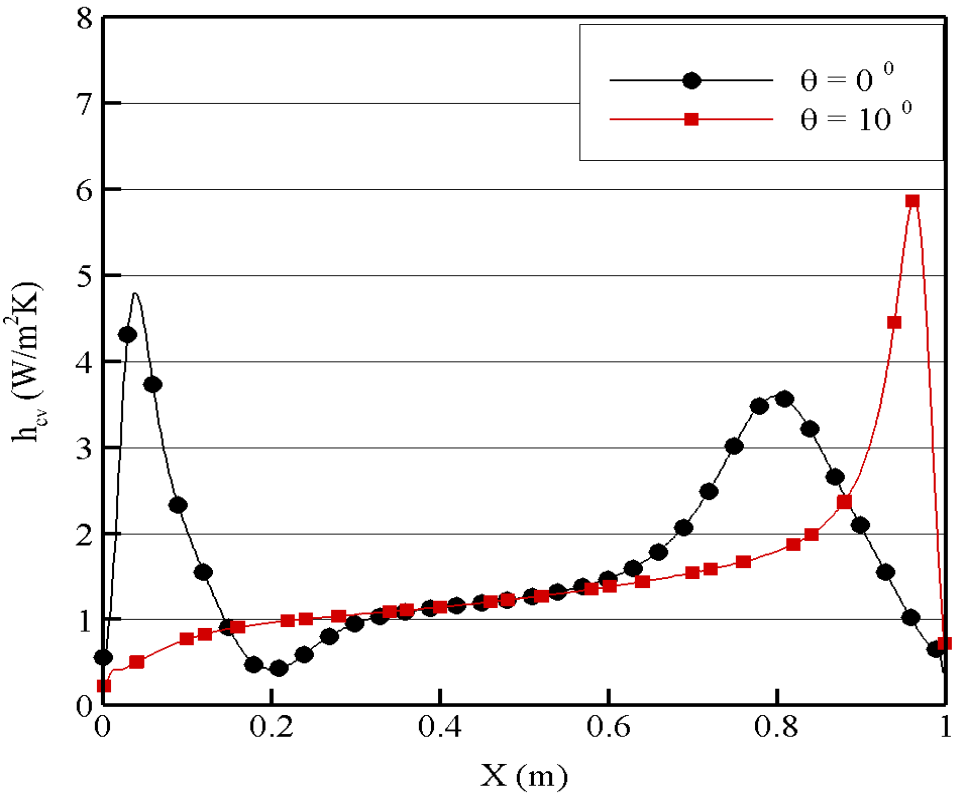

Figure 14. Convective heat transfer coefficient at AR = 5.52; θ = 0°and θ = 10°.

Now, despite the somewhat anomalous behavior with an increase of cover angle at AR = 5.52, an increase in the heat transfer coefficient with cover angle was noticed for all other aspect ratios. To illustrate this point, Figure 15 shows that for an aspect ratio of 3.55, the (local) heat transfer coefficient on the basin surface increases for all cover angles (noting that with the change from 0° to 10° there was a reversal of the flow direction).

Again, this tells us that the cover angle, like aspect ratio, plays a more significant role, in solar stills than has been reported in the literature to date.

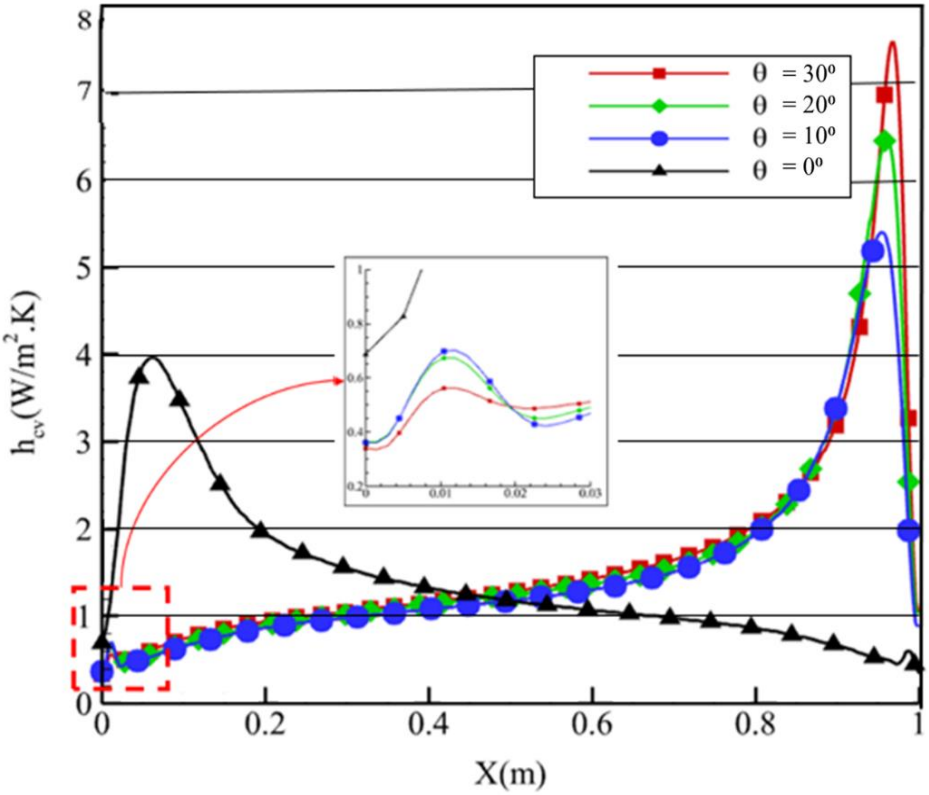

Figure 15. Local heat transfer coefficient for different angles at AR = 3.55.

4.3. Correlating Geometry to Heat and Mass Transfer

The results discussed so far have shown that aspect ratio and the cover surface angle have a significant effect on the convective heat transfer coefficient in a solar still, and this is related to the nature of the flow field. However, to facilitate improved parametric modelling of single slope solar stills, a relationship to describe this would be invaluable.

By generalizing the results from the CFD modelling, the relationship between the Nusselt number and the previous parameters can be represented by a multiparameter correlation, as shown in Equation (3) (where $3.37 \times 10^6 < Ra < 3.03 \times 10^9$; $0^\circ < \theta < 60^\circ$; $1 < AR < 8$).

$$Nu = Ra^{0.187} (AR)^{-0.488} \cos(\theta)^{-0.416} \quad (3)$$

Figure 16 shows that within the range of Rayleigh numbers examined (typical of a solar still), there is a good relationship between the CFD results and the predicted values from the proposed correlation (less than 15% difference). This suggests that the Equation (3) is well suited for use in predicting the heat transfer coefficient for a wide range of geometries.

Now, in Equation (3) only the natural convection heat transfer process of the solar still was accounted for. Sharpley and Boelter [57] noted that for heat transfer alone, the Rayleigh number varies directly with the temperature difference $(T_h - T_c)$. However, in the case of solar stills, mass transfer occurs simultaneously with heat transfer, therefore, the Rayleigh number varies directly with $\Delta T' = \left(\frac{M_c T_c}{M_h T_h} - 1\right)$. For this reason, Equation (2) should be modified to consider the mass transfer process through the use of a 'modified' Rayleigh number. Thus, the proposed correlation can be represented by Equation (4) using the modified form of the Rayleigh number shown in Equation (5).

$$Nu' = Ra'^{0.187} (AR)^{-0.488} \cos(\theta)^{-0.416} \quad (4)$$

where:

$$Ra' = \frac{\rho_a{}^2 g \beta_a \Delta T' C p_a L^3}{\lambda_a \mu_a} \quad (5)$$

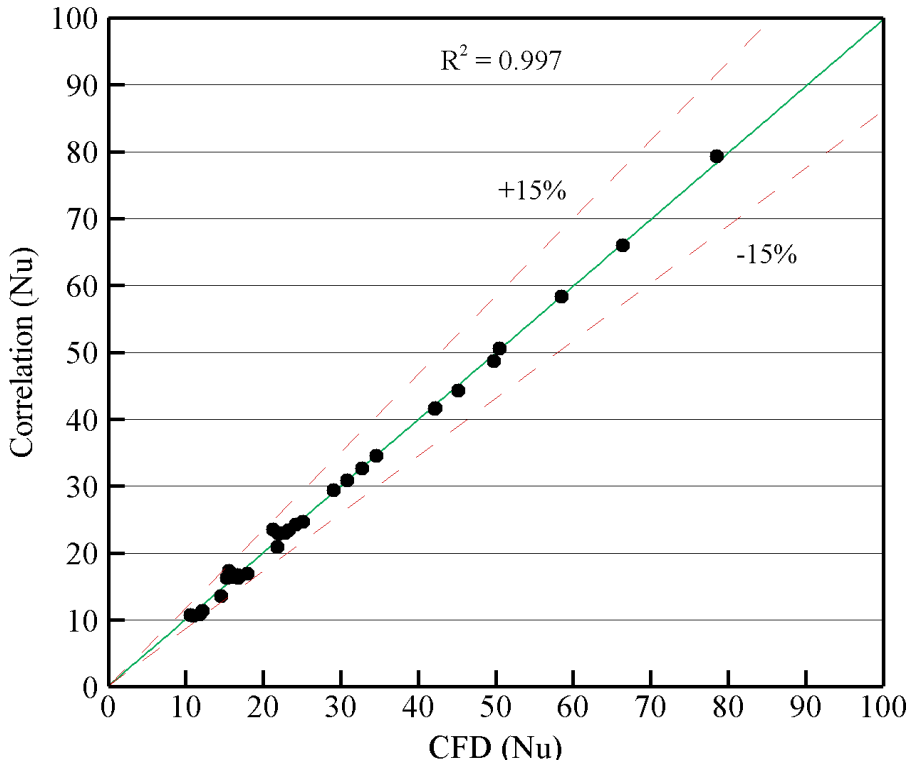

Figure 16. Correlated data of the study.

As an illustration of the effect of the new correlation, a comparison between the Nusselt number from the correlation in this study, and that of the widely used Dunkle relationship is shown in Figure 17. It can be seen that Dunkle's correlation predicts a significantly higher Nusselt number for all cover angles (at a constant aspect ratio), thus explaining part of the reason it fails to accurately predict solar still yield in practice.

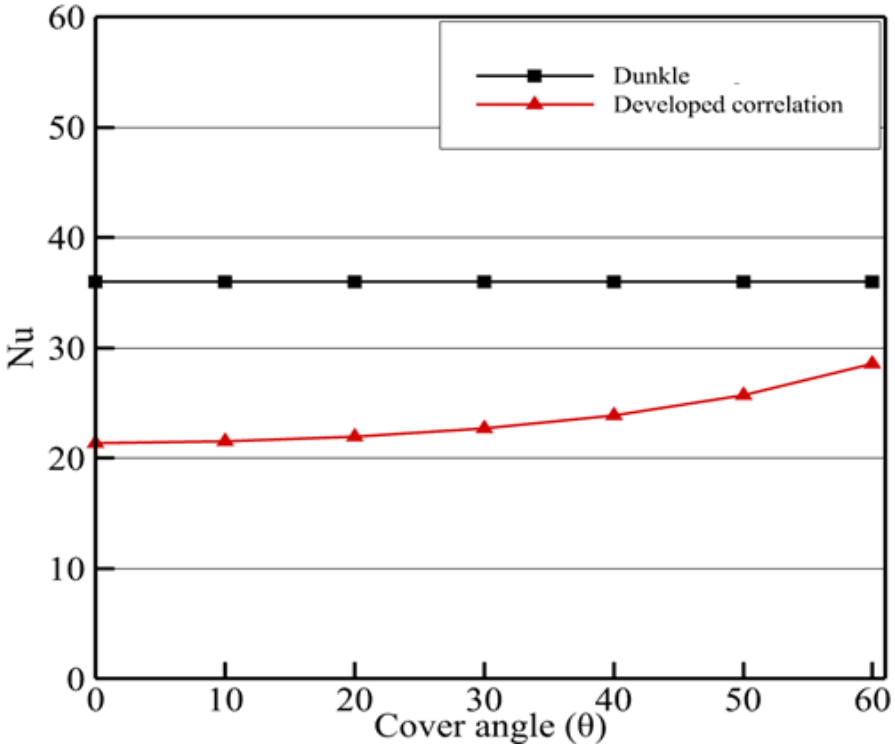

Figure 17. Nusselt number variation for different cover angles at AR = 2.78.

Furthermore, it is apparent that Dunkle's relationship, despite widespread use in its original or modified form, is entirely independent of cover angle. As the angle increases, there is no change in the Nusselt number (at a constant aspect ratio). This also helps clarify the reasons for the contradictory observations reported in the literature relating to the optimum cover angle.

4.4. Verification of the Proposed Correlation Using Independent Experimental Data

Having shown that Dunkle's relationship delivered a poor representation of the transfer processes occurring in a solar still, it was decided to examine the general applicability of the correlation developed in the preceding section. To do this, it was decided to see if the yield of single slope solar stills reported by Shawaqfeh and Farid, Manoj Kumar et al., Attia et al., and Rabhi et al. [28,58–60] (Table 1) could be determined using the temperature difference between the water surface and the glass cover temperature reported in each of these studies. Although the studies all examined single slope solar stills, they had widely differing cover angles (θ), aspect ratios (AR) and temperature differences, thereby providing a good test of the correlation's generalizability.

In Figure 18 it can be seen that the yield obtained using the proposed correlation (Equation (4)) and the experimental measurements from the independent experimental studies are in very close agreement. With less than 5% error in the cumulative yield between the correlation and experimental measurements, it is apparent that the correlation provides an accurate prediction of single slope solar still performance. Moreover, it exhibits greater generalisability than existing correlations.

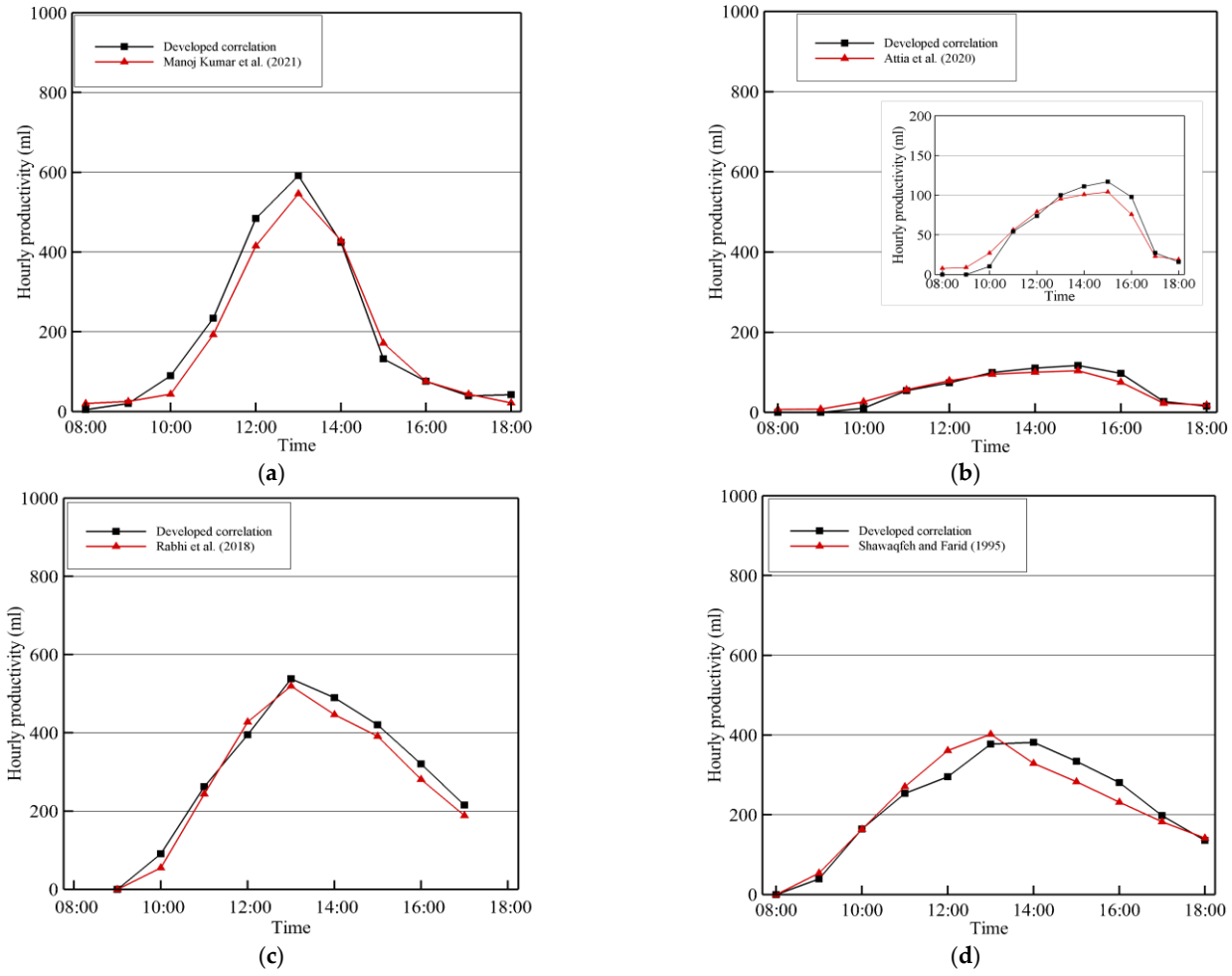

Figure 18. Predicted hourly yield against measured data, (**a**) Manoj Kumar et al. [59], (**b**) Attia et al. [60], (**c**) Rabhi et al. [58], (**d**) Shawaqfeh and Farid [28].

Table 1. Cover angle and aspect ratio for validation studies.

Study	Cover Angle	Aspect Ratio
Rabhi et al. [58]	35°	1.1
Manoj Kumar et al. [59]	11°	1.9
Attia et al. [60]	9°	2.6
Shawaqfeh and Farid [28]	20°	3

5. Conclusions

Despite the long history of research into single slope solar still performance, and their apparent simplicity, a striking absence was the lack of accounting for the possible effects of cover angle and aspect ratio. By taking an unorthodox approach (for solar still research) of decoupling the transfer processes in the still from the operation of the still, this study showed that the natural convection (the primary transport mechanism) was closely linked to both the aspect ratio and the cover angle of the still, as independent parameters.

It was shown that for some conditions, a single convection cell existed, however by varying the cover angle or aspect ratio it was possible to generate additional cells, which in turn encouraged higher heat transfer from the basin to the cover. Furthermore, it was shown that the effect of these changes could be accounted for in the form of a generalized correlation that included cover angle and aspect ratio.

Subsequently, it was shown that the correlation was generalizable and could predict the freshwater yield of several independent experimental studies. As such, where previous models have ignored cover angle and aspect ratio as independent design parameters, this work finally opens the possibility of developing a full design model for single slope solar stills.

Author Contributions: Conceptualization, T.A., R.N. and D.E.B.S.; Methodology, T.A. and D.E.B.S.; Validation, D.E.B.S.; Formal Analysis, D.E.B.S.; Resources, T.A. and R.N.; Writing—Original Draft Preparation, D.E.B.S.; Writing—Review & Editing, T.A.; Supervision, T.A. and R.N. All authors have read and agreed to the published version of the manuscript.

Funding: This research received no external funding.

Acknowledgments: The authors thank the Ministry of Foreign Affairs and Trade, New Zealand for the provision of a scholarship to undertake this work.

Conflicts of Interest: The authors declare no conflict of interest.

Nomenclature

AR	Aspect ratio (B/L)
B	Base width
Cp	Specific heat
g	Gravity
h	Heat transfer coefficient
L	Characteristic length (average enclosure height)
M	Molar weight of air and water vapour mixture
Nu	Nusselt number
Nu′	Modified Nusselt number
Ra	Rayleigh number
Ra′	Modified Rayleigh number
q	Heat flux
T	Temperature
W	Width
ΔT	Temperature difference between water and glass
Δt	Time difference
ΔT′	Modified temperature difference between water and glass
X	X component
Y	Y component

Subscripts

a	Air
c	Cold surface (Glass cover)
cv	Convective
h	Hot surface (Water surface)
s	Silicone oil
t	Total

Greek symbols

μ	Viscosity
λ	Thermal conductivity
β	Volume expansion coefficient
ρ	Density
θ	Inclination angle relative to the horizontal

References

1. Sampathkumar, K.; Arjunan, T.V.; Pitchandi, P.; Senthilkumar, P. Active solar distillation—A detailed review. *Renew. Sustain. Energy Rev.* **2010**, *14*, 1503–1526. [CrossRef]
2. Gude, V.G. Energy storage for desalination processes powered by renewable energy and waste heat sources. *Appl. Energy* **2015**, *137*, 877–898. [CrossRef]
3. Samuel, D.H.; Nagarajan, P.; Sathyamurthy, R.; El-Agouz, S.; Kannan, E. Improving the yield of fresh water in conventional solar still using low cost energy storage material. *Energy Convers. Manag.* **2016**, *112*, 125–134. [CrossRef]
4. Hansen, R.S.; Narayanan, C.S.; Murugavel, K.K. Performance analysis on inclined solar still with different new wick materials and wire mesh. *Desalination* **2015**, *358*, 1–8. [CrossRef]
5. Srivastava, P.K.; Agrawal, S.K. Experimental and theoretical analysis of single sloped basin type solar still consisting of multiple low thermal inertia floating porous absorbers. *Desalination* **2013**, *311*, 198–205. [CrossRef]
6. Panchal, H.N.; Shah, P.K. Effect of Varying Glass cover thickness on Performance of Solar still: In a Winter Climate Conditions. *Int. J. Renew. Energy Res.* **2012**, *1*, 212–223.
7. El-Sebaii, A.; Al-Ghamdi, A.; Al-Hazmi, F.; Faidah, A.S. Thermal performance of a single basin solar still with PCM as a storage medium. *Appl. Energy* **2009**, *86*, 1187–1195. [CrossRef]
8. Abdallah, S.; Abu-Khader, M.M.; Badran, O. Effect of various absorbing materials on the thermal performance of solar stills. *Desalination* **2009**, *242*, 128–137. [CrossRef]
9. Kaushika, N.D.; Sumathy, K. Solar transparent insulation materials: A review. *Renew. Sustain. Energy Rev.* **2003**, *7*, 317–351. [CrossRef]
10. Tiris, Ç.; Tiris, M.; Türe, İ.E. Improvement of basin type solar still performance: Use of various absorber materials and solar collector integration. *Renew. Energy* **1996**, *9*, 758–761. [CrossRef]
11. Elango, C.; Gunasekaran, N.; Sampathkumar, K. Thermal models of solar still—A comprehensive review. *Renew. Sustain. Energy Rev.* **2015**, *47*, 856–911. [CrossRef]
12. Dunkle, R. Solar water distillation: The roof type still and a multiple effect diffusion still. In Proceedings of the International Heat Transfer Conference, University of Colorado, Denver, CO, USA, 28 August–1 September 1961.
13. Rubio, E.; Fernández-Zayas, J.L.; Porta-Gándara, M.A. Current Status of Theoretical and Practical Research of Seawater Single-Effect Passive Solar Distillation in Mexico. *J. Mar. Sci. Eng.* **2020**, *8*, 94. [CrossRef]
14. Porta-Gándara, M.; Fernández-Zayas, J.; Chargoy-del-Valle, N. Solar still distillation enhancement through water surface perturbation. *Sol. Energy* **2020**, *196*, 312–318. [CrossRef]
15. Muñoz, F.; Barrera, E.; Ruiz, A.; Martínez, E.; Chargoy, N. Long-term experimental theoretical study on several single-basin solar stills. *Desalination* **2020**, *476*, 114241. [CrossRef]
16. Khan, M.Z.; Khan, E.H.; Agarhari, N.; Wahid, M.A.; Nawaz, I. Calculation for the Output of Solar Still of an Individual Hour. In *Advances in Materials Engineering and Manufacturing Processes*; Springer: Berlin/Heidelberg, Germany, 2020; pp. 117–130.
17. Hedayatizadeh, M.; Sarhaddi, F.; Pugsley, A. A detailed thermal modeling of a passive single-slope solar still with improved accuracy. *Groundw. Sustain. Dev.* **2020**, *11*, 100384. [CrossRef]
18. El-Sebaii, A.; Khallaf, A.E.-M. Mathematical modeling and experimental validation for square pyramid solar still. *Environ. Sci. Pollut. Res.* **2020**, *27*, 32283–32295. [CrossRef]
19. Dumka, P.; Mishra, D.R. Performance evaluation of single slope solar still augmented with the ultrasonic fogger. *Energy* **2020**, *190*, 116398. [CrossRef]
20. Dumka, P.; Mishra, D.R. Influence of salt concentration on the performance characteristics of passive solar still. *Int. J. Ambient. Energy* **2019**, *42*, 1463–1473. [CrossRef]
21. Agrawal, A.; Rana, R. Theoretical and experimental performance evaluation of single-slope single-basin solar still with multiple V-shaped floating wicks. *Heliyon* **2019**, *5*, e01525. [CrossRef]

22. Sivakumar, V.; Sundaram, E.G.; Sakthivel, M. Investigation on the effects of heat capacity on the theoretical analysis of single slope passive solar still. *Desalination Water Treat.* **2016**, *57*, 9190–9202. [CrossRef]
23. El-Sebaii, A.; Al-Dossari, M. A mathematical model of single basin solar still with an external reflector. *Desalination Water Treat.* **2011**, *26*, 250–259. [CrossRef]
24. Feilizadeh, M.; Soltanieh, M.; Jafarpur, K.; Estahbanati, M.R.K. A new radiation model for a single-slope solar still. *Desalination* **2010**, *262*, 166–173. [CrossRef]
25. Shukla, S.; Sorayan, V. Thermal modeling of solar stills: An experimental validation. *Renew. Energy* **2005**, *30*, 683–699. [CrossRef]
26. Fath, H.E.; Elsherbiny, S.M. Effect of adding a passive condenser on solar still performance. *Int. J. Sol. Energy* **1992**, *11*, 73–89. [CrossRef]
27. McAdams, W.H. *Heat Transmission*, 3rd ed.; McGraw Hill: New York, NY, USA, 1954; p. 181.
28. Shawaqfeh, A.T.; Farid, M.M. New development in the theory of heat and mass transfer in solar stills. *Sol. Energy* **1995**, *55*, 527–535. [CrossRef]
29. Yilmaz, T.P.; Aybar, H.S. *Evaluation of the Correlations for Predicting Evaporative Loss from Water Body*; American Society of Heating, Refrigerating and Air-Conditioning Engineers, Inc.: Atlanta, GA, USA, 1999.
30. Hongfei, Z.; Xiaoyan, Z.; Jing, Z.; Yuyuan, W. A group of improved heat and mass transfer correlations in solar stills. *Energy Convers. Manag.* **2002**, *43*, 2469–2478. [CrossRef]
31. Rahbar, N.; Esfahani, J.A. Estimation of convective heat transfer coefficient in a single-slope solar still: A numerical study. *Desalination Water Treat.* **2012**, *50*, 387–396. [CrossRef]
32. Rahbar, N.; Esfahani, J.A. Productivity estimation of a single-slope solar still: Theoretical and numerical analysis. *Energy* **2013**, *49*, 289–297. [CrossRef]
33. Jamil, B.; Akhtar, N. Effect of specific height on the performance of a single slope solar still: An experimental study. *Desalination* **2017**, *414*, 73–88. [CrossRef]
34. Keshtkar, M.; Eslami, M.; Jafarpur, K. Effect of design parameters on performance of passive basin solar stills considering instantaneous ambient conditions: A transient CFD modeling. *Sol. Energy* **2020**, *201*, 884–907. [CrossRef]
35. Tsilingiris, P.T. The influence of binary mixture thermophysical properties in the analysis of heat and mass transfer processes in solar distillation systems. *Sol. Energy* **2007**, *81*, 1482–1491. [CrossRef]
36. Tiwari, G.; Minocha, A.; Sharma, P.; Khan, M. Simulation of convective mass transfer in a solar distillation process. *Energy Convers. Manag.* **1997**, *38*, 761–770. [CrossRef]
37. Adhikari, R.S.; Kumar, A.; Kumar, A. Estimation of mass-transfer rates in solar stills. *Int. J. Energy Res.* **1990**, *14*, 737–744. [CrossRef]
38. Sharon, H.; Reddy, K.S.; Krithika, D.; Philip, L. Experimental performance investigation of tilted solar still with basin and wick for distillate quality and enviro-economic aspects. *Desalination* **2017**, *410*, 30–54. [CrossRef]
39. Murugavel, K.K.; Chockalingam, K.K.S.K.; Srithar, K. Progresses in improving the effectiveness of the single basin passive solar still. *Desalination* **2008**, *220*, 677–686. [CrossRef]
40. Samee, M.A.; Mirza, U.K.; Majeed, T.; Ahmad, N. Design and performance of a simple single basin solar still. *Renew. Sustain. Energy Rev.* **2007**, *11*, 543–549. [CrossRef]
41. Agrawal, A.; Rana, R.S.; Srivastava, P.K. Heat transfer coefficients and productivity of a single slope single basin solar still in Indian climatic condition: Experimental and theoretical comparison. *Resour. Effic. Technol.* **2017**, *3*, 466–482. [CrossRef]
42. Nougriaya, S.K.; Chopra, M.; Gupta, B.; Baredar, P. Stepped solar still: A review on designs analysis. *Mater. Today Proc.* **2020**, *46*, 5647–5660. [CrossRef]
43. Khalifa, A.J.N. On the effect of cover tilt angle of the simple solar still on its productivity in different seasons and latitudes. *Energy Convers. Manag.* **2011**, *52*, 431–436. [CrossRef]
44. Tiwari, G.; Thomas, J.; Khan, E. Optimisation of glass cover inclination for maximum yield in a solar still. *Heat Recovery Syst. CHP* **1994**, *14*, 447–455. [CrossRef]
45. Setoodeh, N.; Rahimi, R.; Ameri, A. Modeling and determination of heat transfer coefficient in a basin solar still using CFD. *Desalination* **2011**, *268*, 103–110. [CrossRef]
46. Hammami, M.; Mseddi, M.; Baccar, M. Numerical Study of Coupled Heat and Mass Transfer in a Trapezoidal Cavity. *Eng. Appl. Comput. Fluid Mech.* **2007**, *1*, 216–226. [CrossRef]
47. Omri, A.; Orfi, J.; Nasrallah, S.B. Natural convection effects in solar stills. *Desalination* **2005**, *183*, 173–178. [CrossRef]
48. Rincón-Casado, A.; De La Flor, F.S.; Vera, E.C.; Ramos, J.S.; De La Flor, F.J.S. New natural convection heat transfer correlations in enclosures for building performance simulation. *Eng. Appl. Comput. Fluid Mech.* **2017**, *11*, 340–356. [CrossRef]
49. Zheng, H. *Solar Energy Desalination Technology*; Elsevier: Amsterdam, The Netherlands, 2017.
50. Tiwari, G.N.; Sahota, L. General Introduction. In *Advanced Solar-Distillation Systems: Basic Principles, Thermal Modeling, and Its Application*; Tiwari, G.N., Sahota, L., Eds.; Springer: Singapore, 2017; pp. 1–62.
51. Flack, R.D. The Experimental Measurement of Natural Convection Heat Transfer in Triangular Enclosures Heated or Cooled from Below. *J. Heat Transf.* **1980**, *102*, 770–772. [CrossRef]
52. Poulikakos, D.; Bejan, A. Natural Convection Experiments in a Triangular Enclosure. *J. Heat Transf.* **1983**, *105*, 652–655. [CrossRef]
53. Altaç, Z.; Uğurlubilek, N. Assessment of turbulence models in natural convection from two- and three-dimensional rectangular enclosures. *Int. J. Therm. Sci.* **2016**, *107*, 237–246. [CrossRef]

54. Nijegorodov, N.; Jain, P.K.; Carlsson, S. Thermal-electrical, high efficiency solar stills. *Renew. Energy* **1994**, *4*, 123–127. [CrossRef]
55. *Fluent, User Manual Release 16.1*; ANSYS Inc.: Canonsburg, PA, USA, 2015.
56. Raffel, M.; Willert, C.E.; Scarano, F.; Kähler, C.J.; Wereley, S.T.; Kompenhans, J. *Particle Image Velocimetry: A Practical Guide*; Springer: Berlin/Heidelberg, Germany, 2018.
57. Sharpley, B.; Boelter, L. Evaporation of water into quiet air from a one-foot diameter surface. *Ind. Eng. Chem.* **1938**, *30*, 1125–1131. [CrossRef]
58. Rabhi, K.; Nciri, R.; Nasri, F.; Ali, C.; Ben Bacha, H. Experimental performance analysis of a modified single-basin single-slope solar still with pin fins absorber and condenser. *Desalination* **2017**, *416*, 86–93. [CrossRef]
59. Kumar, P.M.; Sudarvizhi, D.; Prakash, K.; Anupradeepa, A.; Raj, S.B.; Shanmathi, S.; Sumithra, K.; Surya, S. Investigating a single slope solar still with a nano-phase change material. *Mater. Today Proc.* **2021**, *45*, 7922–7925. [CrossRef]
60. Attia, M.E.H.; Hussein, A.K.; Rout, S.K.; Soli, J.; Elaloui, E.; Driss, Z.; Ghougali, M.; Kolsi, L.; Chand, R. Experimental Study of the Effect of Al_2O_3 Nanoparticles on the Profitability of a Single-Slope Solar Still: Application in Southeast of Algeria. In *Advances in Air Conditioning and Refrigeration*; Springer: Berlin/Heidelberg, Germany, 2021; pp. 119–133.